TRANSNAV International Journal on Marine Navigation and Safety of Sea Transportation
Volume 6 Number 1 March 2012

Research on Ship Navigation in Numerical Simulation of Weather and Ocean in a Bay

T. Soda
Kobe University, Faculty of Maritime Sciences
S. Shiotani
Kobe University, Organization of Advanced Science and Technology
H. Makino & Y. Shimada
Kobe University, Faculty of Maritime Sciences

ABSTRACT: For safe navigation, high-resolution information on tidal current, wind and waves is very important. In coastal areas in particular, the weather and ocean situation change dramatically in time and place according to the effects of geography and water depth. In this paper, high-resolution wave data was generated using SWAN as a numerical wave model. To estimate waves, wind data is necessary. By using the mesoscale meteorological model of WRF-ARW, detailed wind data was generated. The tidal current data was generated by using POM.
We simulated tidal currents, wind and ocean waves for the duration of a typhoon passing over Japan in September of 2004.
Secondly, we simulated ship maneuvering using simulated tidal current, wind and wave data. For the ship maneuvering model, the MMG (Mathematic Modeling Group) was used. Combining high-resolution tidal current, wind and wave data with the numerical navigation model, we studied the effects of tidal current, wind and waves on a ship's maneuvering. Comparing the simulated route lines of a ship with the set course, it was recognized that the effects of the tidal current, wind and waves on a moving ship were significant.

1 INTRODUCTION

Winds, tidal currents, and waves of the ocean are considered the most important factors in the field of ocean engineering. In particular, the numerical forecasting of tidal currents, winds over the sea, and ocean waves in coastal areas is important for ocean environments, fisheries, and navigation. In the previous paper[1][2], the numerical simulation of tidal currents as they relate to the winds in a bay was explained. The simulation of tidal currents was carried out in Japan's Osaka Bay. Detailed tidal currents were calculated using the POM (Princeton Oceanography Model). The results of the numerical simulation of tidal currents and tidal elevations were compared with data from observations in the bay. A comparison of the numerical and calculated results showed agreement.

In this paper, a numerical simulation of winds on the sea was carried out in Japan's Osaka Bay area. Details of the distribution of winds on the sea were calculated using the WRF model developed principally by National Centers for Environmental Prediction (NCEP) and National Oceanic and Atmospheric Administration (NOAA) in the United States. The wind calculation was continued for 4 days while a typhoon passed over the Nihon Sea near Japan. A strong wind blew from the south on the coastal sea area. The simulation of ocean waves was carried out in the same bay area where the wind simulation was done, and the calculated wind and tidal currents were used. Details of the distribution of waves on the sea were calculated using the SWAN[3][4] (Simulating WAves Nearshore) model developed at Delft University of Technology in the Netherlands. The simulation of tidal currents was calculated using the POM numerical model. We analyzed wind stress on tidal current by using WRF-calculated wind data.

Secondly, the numerical simulation of winds and waves was applied to a navigational simulation of a sailing ship in the bay area.

The accurate estimation of a given ship's position is very important for optimal ship routing[5]. Such estimations can be obtained when the hydrodynamic model, which is widely used to describe a ship's maneuvering motion, is adopted in order to estimate a ship’s position. As a first step toward this final objective of optimum routing, the effects of winds, waves, and tidal currents on a ship's maneuverability were examined through numerical simulations.

2 NUMERICAL SIMULATION OF OCEAN WINDS

The simulation of winds was carried out by WRF-ARW3.1.1, a mesoscale meteorological model developed principally among the National Center for Atmospheric Research (NCAR), the National Oceanic and Atmospheric Administration (NOAA), the National Centers for Environmental Prediction (NCEP), the Forecast Systems Laboratory (FSL), the Air Force Weather Agency (AFWA), the Naval Research Laboratory, the University of Oklahoma, and the Federal Aviation Administration (FAA).

The equation set for WRF-ARW is fully compressible, Eulerian, and nonhydrostatic, with a runtime hydrostatic option. The time integration scheme in the model uses the third-order Runge-Kutta scheme, and the spatial discretization employs second- to sixth-order schemes.

GFS-FNL data were used as boundary data[6]. The Global Forecast System (GFS) is operationally run four times a day in near-real time at NCEP. GFS-FNL (Final) Operational Global Analysis data are set on 1.0 x 1.0 degree grids every 6 hours.

The simulated term was 96 hours from 5 September, 2004, 00:00 UTC to 9 September, 2004, 00:00 UTC. Figure 1 shows the weather charts of the simulated term. In this figure, (b) shows the typhoon located over the southwest of Japan on 7 September 00:00 UTC, and (c) shows the area after the typhoon had passed on 8 September 00:00 UTC.

Two areas for nesting were calculated in order to simulate winds accurately. While the typhoon was passing over Japan, a strong south wind blew on the Japanese Pacific side. Figure 2 shows the two areas, d01 and d02. The center point of d01 is E135.52 N34.72.

The numerical simulation of wind was carried out in the area around Japan. The grid numbers are 44 x 35 x 28 in the x-y-z axis in d01 and 41 x 36 x 28 in the x-y-z axis in d02. The horizon grid intervals of Δx and Δy are 10 km in d01 and 2 km in d02. In both areas, the vertical grid is 20 from top pressure (500 Pa) to ground pressure. The condition calculated by WRF is shown in Table 1.

At the points shown in Figure 3, the calculated wind data were verified by the wind observed with the AmeDAS, the system of the Japan Meteorological Agency. The results of wind simulation at these points are shown in Figure 4. The horizontal axis shows the time from the start time of calculation in hours. The vertical axis shows the wind velocity and wind direction.

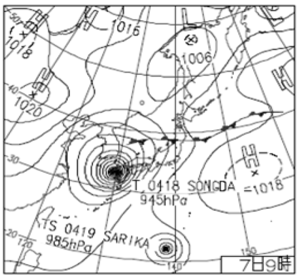

(a) 6 Sept. 2004 00:00 UTC

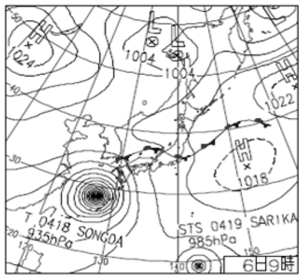

(b) 7 Sept. 2004 00:00 UTC

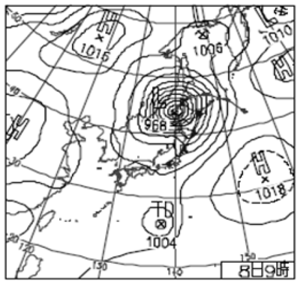

(c) 8 Sept. 2004 00:00UTC

Figure 1. Chart of calculation term

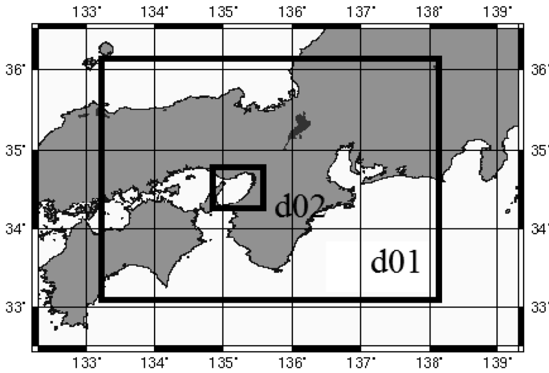

Figure 2. Two calculation areas

Table 1. Condition of calculations by WRF

	d01	d02
Dimension	44 x 35 x 28	41 x 36 x 28
Mesh size	10 (km)	2 (km)
Time step	60 (s)	12 (s)
Start time	2004-09-05-00:00:00 UTC	
End time	2004-09-09-00:00:00 UTC	

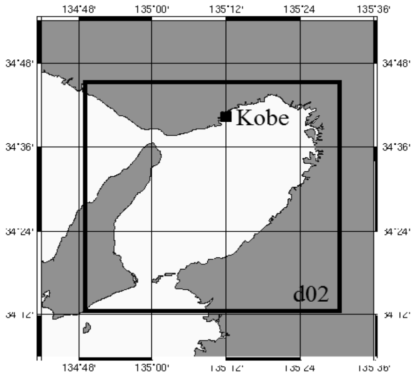

Figure 3. The comparison points for wind, tide level and wave height

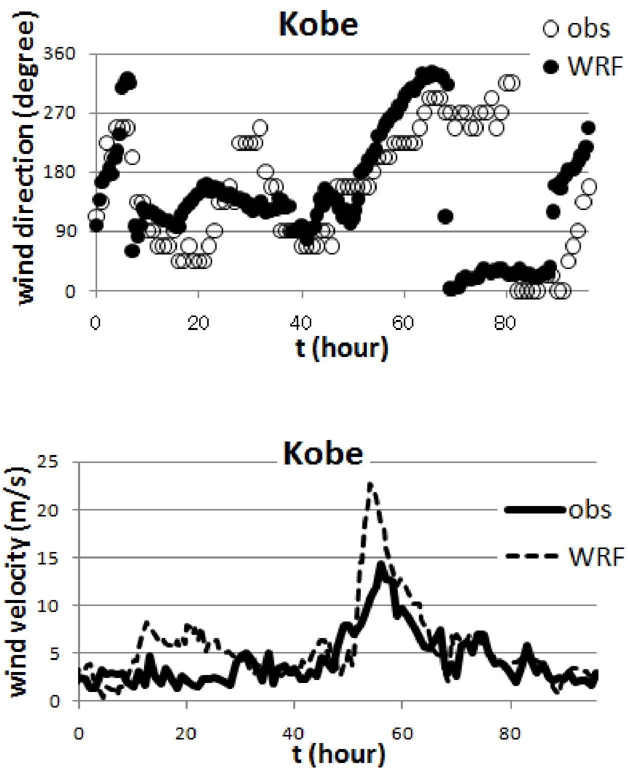

Figure 4. Comparison of calculated and observed wind velocities and directions

The results of the wind simulation are shown in Figure 4. In the time when the typhoon was closest, the estimated wind velocity is lower than the observed data at the point in Kobe. The RMS error of wind velocity is 2.3 m/s, and the correlation coefficient of wind velocity is 0.89. The simulation of wind is generally estimated accurately.

3 NUMERICAL SIMULATION OF TIDAL CURRENT

The estimation of tidal current was carried out by using the Princeton Oceanographic Model (POM) (Mellor 2004). The basic equations of the tidal current are the continuity equation and Navier-Stokes equation, shown as follows:

$$\frac{\partial DU}{\partial x}+\frac{\partial DV}{\partial y}+\frac{\partial \omega}{\partial \sigma}+\frac{\partial \eta}{\partial t}=0 \tag{1}$$

$$\frac{\partial UD}{\partial t}+\frac{\partial U^2 D}{\partial x}+\frac{\partial UVD}{\partial y}+\frac{\partial U\omega}{\partial \sigma}-fVD+gD\frac{\partial \eta}{\partial x}+\frac{gD^2}{\rho_0}\int_\sigma^0\left[\frac{\partial \rho'}{\partial x}-\frac{\sigma'}{D}\frac{\partial D}{\partial x}\frac{\partial \rho'}{\partial \sigma'}\right]d\sigma'=\frac{\partial}{\partial \sigma}\left[\frac{K_M}{D}\frac{\partial U}{\partial \sigma}\right]+F_x \tag{2}$$

$$\frac{\partial UD}{\partial t}+\frac{\partial UVD}{\partial x}+\frac{\partial V^2 D}{\partial y}+\frac{\partial V\omega}{\partial \sigma}+fUD+gD\frac{\partial \eta}{\partial y}+\frac{gD^2}{\rho_0}\int_\sigma^0\left[\frac{\partial \rho'}{\partial y}-\frac{\sigma'}{D}\frac{\partial D}{\partial y}\frac{\partial \rho'}{\partial \sigma'}\right]d\sigma'=\frac{\partial}{\partial \sigma}\left[\frac{K_M}{D}\frac{\partial V}{\partial \sigma}\right]+F_y \tag{3}$$

where (u and v) are the components of the horizontal velocity of tidal current, ω is the velocity component of the normal direction to the σ plain, f is the Coriolis coefficient, g is the acceleration of gravity, F_x and F_y are the horizontal viscosity diffusion coefficients, and KM is the frictional coefficient of the sea bottom.

We calculated the effect of wind stress on tidal current by using wind data gathered by WRF. The grid number is 328 x 288 in the x-y axis in d02. The horizon grid interval of Δx and Δy is 250 m in d02. The calculation time interval was 2 seconds.

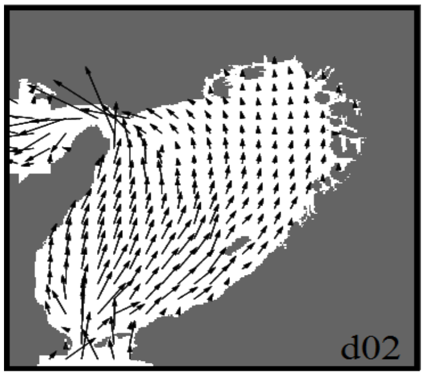

(a) Flow 2004-09-07 04:00 UTC

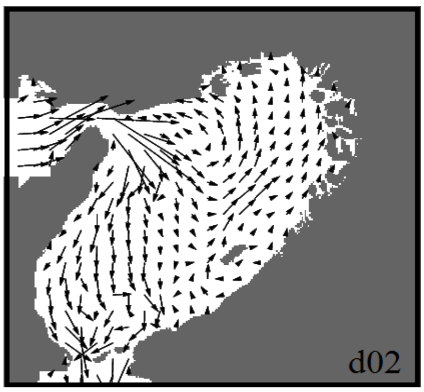

(b) Ebb 20040907 11:00 UTC

Figure 5. Distribution of calculated tidal current on the surface of the sea

Figure 5. Surface tidal current when the typhoon was closest. A comparison of flow and ebb shows that the direction of the tidal current was changed dramatically.

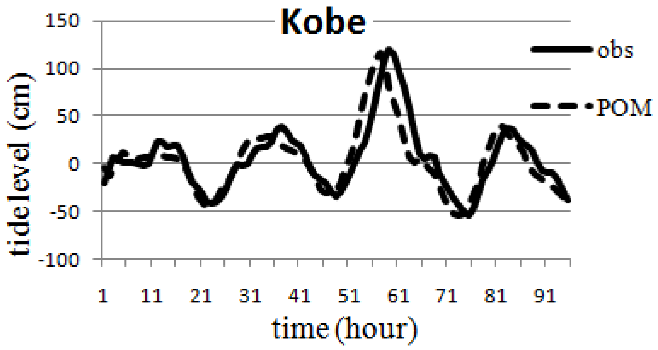

Figure 6. Comparison of calculated and observed tidal level

The tidal level of the simulated and observation in Kobe are shown in Figure 4. The tidal level during the typhoon's approach was higher by strong southern wind. The tidal level was estimated accuracy.

4 NUMERICAL SIMULATION OF OCEAN WAVES

As a numerical model for simulating waves, we used SWAN, a third-generation wave simulation model developed at Delft University of Technology.

The SWAN model is used to solve spectral action balance equations without any prior restriction on the spectrum for the effects of spatial propagation, refraction, reflection, shoaling, generation, dissipation, and nonlinear wave-wave interactions. For the SWAN model, the code used was the same as that used for the WAM model. The WAM model calculates problems in deep water on an oceanic scale, and SWAN considers problems from deep water to the surf zone. Consequently, the SWAN model is suitable for estimating waves in bays as well as in coastal regions with shallow water and ambient currents.

Information about the sea surface is contained in the wave variance spectrum or energy density $E(\sigma,\theta)$. Wave energy is distributed over frequencies σ and propagation directions θ. σ is observed in a frame of reference moving with the current velocity, and θ is the direction normal to the wave crest of each spectral component. The action balance equation of the SWAN model in Cartesian coordinates is as follows:

$$\frac{\partial N}{\partial t}+\frac{\partial}{\partial x}(C_x N)+\frac{\partial}{\partial y}(C_y N)+\frac{\partial}{\partial \sigma}(C_\sigma N)+\frac{\partial}{\partial \theta}(C_\theta N) = \frac{S}{\sigma} \tag{4}$$

where the right-hand side contains S, which is the source/sink term that represents all physical processes which generate, dissipate, or redistribute wave energy. The equation of S is as follows:

$$S = S_{in} + S_{ds,w} + S_{ds,b} + S_{ds,br} + S_{nl4} + S_{nl3} \tag{5}$$

in the right-hand side, where S_{in} is the transfer of wind energy to the waves, $S_{ds,w}$ is the energy of whitecapping, $S_{ds,b}$ is the energy of bottom friction, and $S_{ds,br}$ is the energy of depth-induced breaking.

The numerical simulation of waves was carried out in d02. The grid number is 164 x 144 in the x-y axis in d02. The grid interval of Δx and Δy is 500 m in d02. The conditions for calculation by SWAN are shown in Table 2. Figure 7 is a flowchart of wave calculations.

The results of wave simulation, shown in Figure 8, include the significant wave height developing during the typhoon's approach. Comparing the simulation with the observation, we can say that the simulation by SWAN with WRF and POM agrees.

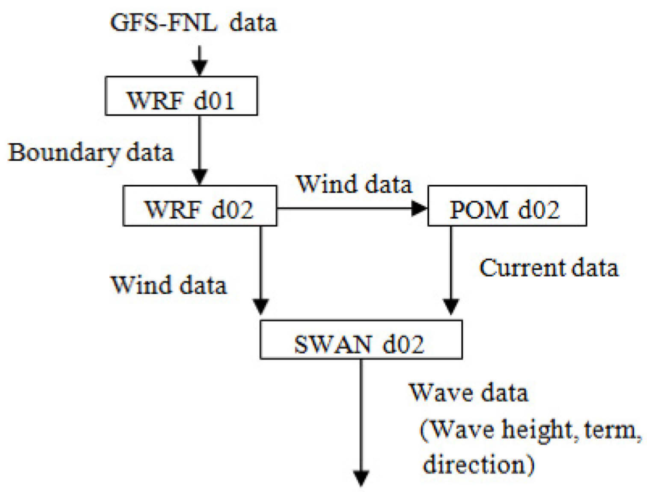

Figure 7. Flow chart for wave calculation by SWAN

Table 2. Conditions for calculations by SWAN

	d02
Dimension	164 x 144
Mesh size	500 (m)
Time step	15 (min)
Start time	2004-09-05-00:00:00 UTC
End time	2004-09-09-00:00:00 UTC
Number of frequencies	30 (0.04Hz-1Hz)
Number of meshes in θ	36

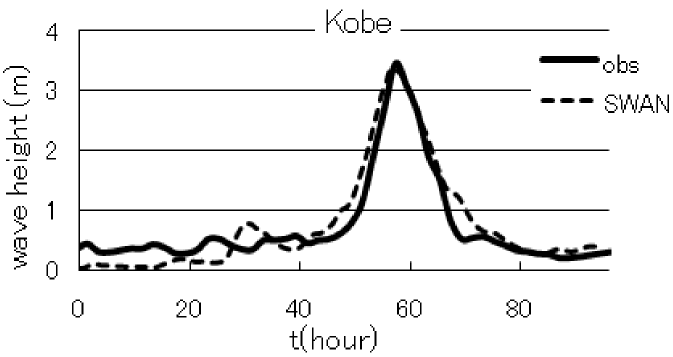

Figure 8. Comparison of calculated and observed wave heights

5 SHIP MANEUVERING SIMULATION

The accurate estimation of a ship's position is very important for optimum ship routing. Such estimations can be obtained when hydrodynamic forces and moments affecting the hull are known in advance. The MMG (Mathematical Model Group) model, widely used to describe a ship's maneuvering motion, was adopted for the estimation of a ship's location by simulation[7]. The primary feature of the MMG model is the division of all hydrodynamic forces and moments working on the vessel's hull, rudder, propeller, and other categories, as well as the analysis of their interaction. The coordinate system is denoted in Figure 9.

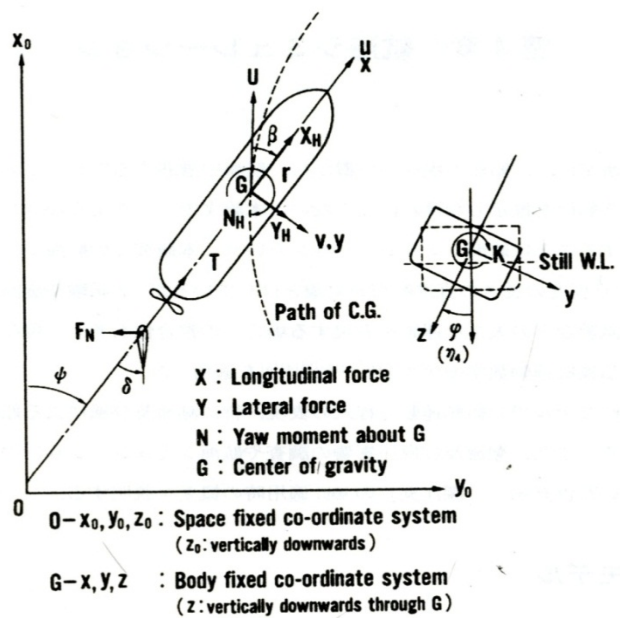

Figure 9. MMG coordinate system

Two coordinate systems, space-fixed and body-fixed, are used in ship maneuverability research. The latter system, G-x,y,z, moves together with the ship and is used in the MMG model. In this coordinate system, G is the center of gravity of the ship, the x-axis is in the direction of the ship's course, the y-axis is perpendicular to the x-axis on the right-hand side, and the z-axis runs downward vertically through G.

Therefore, the equation for the ship's motion in the body-fixed coordinate system adopted in the MMG model is written as follows:

$$\begin{aligned}&(m+m_x)\dot{u}-(m+m_y)vr=X\\&(m+m_y)\dot{v}+(m+m_x)ur=Y\\&(I_{zz}+J_{zz})\dot{r}=N\end{aligned}\qquad(6)$$

where m is the mass, the m_X and m_Y areas are the added mass, and u and v are the components of the velocity in the direction of the x-axis and y-axis, respectively. r is the angular acceleration. I_{ZZ} and J_{ZZ} are the moment of inertia and the added moment of inertia around G, respectively. X and Y are the hydrodynamic forces, and N is the moment around the z-axis.

According to the MMG model, the hydrodynamic force and the moment in the above equation can be shown as follows:

$$\begin{aligned}&X=X_H+X_P+X_R+X_A+X_W+X_E\\&Y=Y_H+Y_P+Y_R+Y_A+Y_W+Y_E\\&N=N_H+N_P+N_R+N_A+N_W+N_E\end{aligned}\qquad(7)$$

where the subscripts *H, P, R, A*, *W* and *E* denote the hydrodynamic force or moment induced by the hull, propellar, rudder, air, waves and external forces, respectively.

The hydrodynamic forces caused by wind are defined in Equation (8):

$$\begin{aligned}&X_A=\frac{\rho_A}{2}V_A^2A_TC_{XA}(\theta_A)\\&Y_A=\frac{\rho_A}{2}V_A^2A_LC_{YA}(\theta_A)\\&N_A=\frac{\rho_A}{2}V_A^2LA_LC_{NA}(\theta_A)\end{aligned}\qquad(8)$$

where ρ_A is the density of air, θ_A is the relative wind direction, V_A is the relative wind velocity, and A_T and A_L are the frontal projected area and the lateral projected area, respectively. C_{XA} , C_{YA} , and C_{NA} are the coefficients, which were estimated by the method of Fujiwara et al.[8]

The hydrodynamic forces caused by waves are defined as follows:

$$\begin{aligned}&X_W=\rho gh^2B^2/L\overline{C_{XW}}(U,T_V,\chi-\psi_0)\\&Y_W=\rho gh^2B^2/L\overline{C_{YW}}(\omega_0,\chi-\psi_0)\\&N_W=\rho gh^2B^2/L\overline{C_{NW}}(\omega_0,\chi-\psi_0)\end{aligned}\qquad(9)$$

where ρ is the density of seawater, g is the acceleration of gravity, h is the amplitude of significant wave height, B is the ship's breadth, L is the length of the ship, and $\overline{C_{XW}}$, $\overline{C_{YW}}$, and $\overline{C_{NW}}$ are averages of short-term estimated coefficients. The hydrodynamic force on the hull surface, including the added resistance, wave-induced steady lateral force, and yaw moment, was obtained through the Research Institute on Oceangoing Ships (RIOS) at the Institute of Naval Architecture, Osaka University. The RIOS was established for the purpose of improving the performance of ships in wind and waves[9].

The frequency-domain response characteristics of wave-induced ship motions with six degrees of freedom were computed using the principal proporties, arrangement plan, and body plan of the ship. In the RIOS system, the wind wave is represented by the ITTC spectrum, and the swell is represented by the JONSWAP spectrum. In this study, the average added resistances, wave-induced steady lateral forces, and yaw moments to the ship by wind-wave and swell are combined.

We simulated the maneuvering of the training ship *Fukaemaru*, the main characteristics of which are shown in Table 3. The relevant data describing the manoevering is shown in reference 2. The starting point of the maneuvering simulation was N34.4 E150, and the set course was 50 degrees. The term of simulation was 4800 seconds from 2004-09-08 05:00:00 UTC. Figure 10 shows the distribution of the tidal current at 2004-09-08 05:00:00 UTC and set ship course. The numerical navigation was carried out at a fixed propeller revolution of 9.0 kn in still water (revolution is 500 rpm).

Table 3. Main characteristics of Fukaemaru

Loa	49.95 m
Lpp	45.00 m
Breadth	10.00 m
Depth	6.10 m
Draft	3.20 m
Gross Tonnage	449 ton
Main Engine Output	1,100 kw
Trial Speed	14.28 knots
Sea Speed	12.50 knots
Steering Engine	3.7 kw

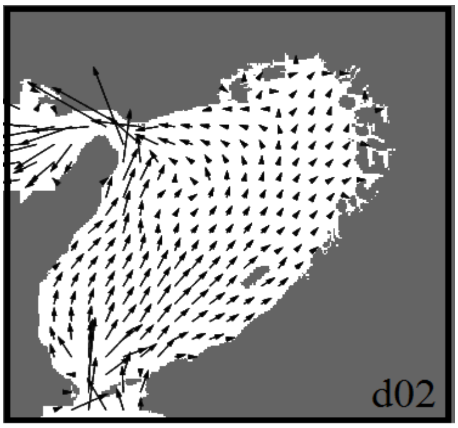

Figure 10. Distribution of tidal current at 2004-09-08 05:00 UTC and ship course

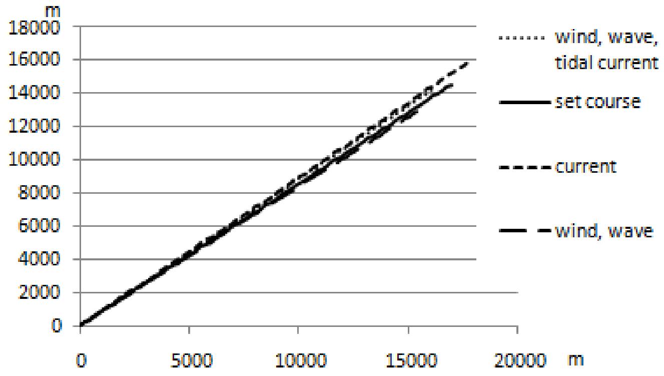

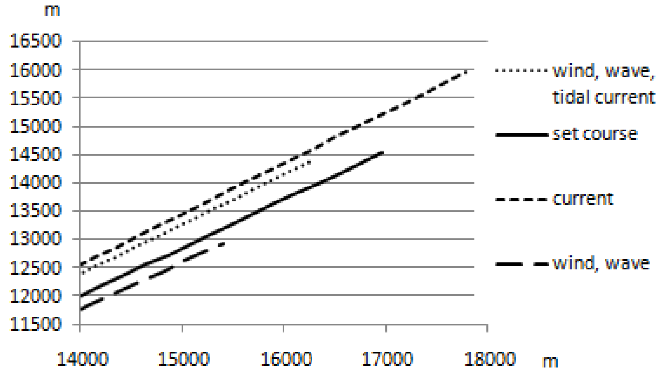

Figure 11. Comparison of wind, wave, and tidal current effect

Figure 11 is the simulated ship course from the start point. In the illustrations below Figure 11, the lower illustration magnifies the rectangular area of the upper one. Each line shows the track based on the effects of "wind and wave," "tidal current," "wind, wave, and tidal current," and the route setting. The results of the numerical navigation, including the effects of winds, waves, and tidal currents, were examined.

6 CONCLUSION

In the present basic study of a numerical navigation system for an oceangoing ship in a bay area, the effects of winds, waves, and tidal currents were studied. The main conclusions are as follows:

1 By combining the numerical models of WRF, POM and SWAN, accurate, high-resolution tidal current, wind and wave data were generated.
2 By using the detailed data, wind and wave force upon the ship was estimated.
3 Detailed data on winds, waves, and tidal currents were applied to a numerical navigation model with estimations of force upon a sailing ship.
4 The effects of winds, waves, and tidal currents on a ship's maneuverability were significant.

With the above information, it is possible to achieve an optimum route by utilizing a numerical simulation if winds, waves, and tidal currents can be predicted in a bay area.

REFERENCES

[1] Xia H., Shiotani S., et al. (2005). A Study of Weather Routing Considering Real Time Data of Weather and Ocean for Sailing Ship in Coastal Area – Basic Simulation of Ship Positioning by Ship Maneuvering and Experiment by a Real Ship, Journal of the Kansai Society of Naval Architects, Japan, No. 234, pp. 159-166.

[2] Xia H., Shiotani S., et al. (2006). Estimation of Ship's Course for Sailing on Route by Navigation Simulation in Coastal Water, The Journal of Japan Institute of Navigation, No. 115, pp. 51-57.

[3] Booji N., et al. (1999). A Third-generation Wave Model for Coastal Regions, Part Ⅰ, Model Description and Validation, J. Geograph. Research, 104, C4, 7649-7666.

[4] The SWAN Team (2009). SWAN, Scientific and Technical Documentation, SWAN Cycle Ⅲ version 40.72ABC, http:/www.swan.tudelft.nl, Delft University of Technology.

[5] Shimada Y., Shiotani S., Takahashi K. (2010). Influence of Ocean Model Horizontal Resolution on Weather Routing, Techno-ocean, CD

[6] Mase H., Katsui S., Yasuda T., Tomand T. H., Ogawa K. (2006). Verification of GFS-WRF-SWAN Wave Prediction System by Three Seasons' Comparison, Annual Journal of Civil Engineering in the Ocean, JSCE VOL. 22, pp. 109-114.

[7] Yoshimura Y. (1986). Mathematical Model for the Maneuvering Ship Motion in Shallow Water, Journal of the Kansai Society of Naval Architects, Japan, No. 200, pp. 41-51.

[8] Fujiwara T., Ueno M., Nimura T. (1998). Estimation of Wind Forces and Moments Acting on Ships, Journal of the Society of Naval Architects of Japan (183), 1998-06, pp. 77-90.

[9] The Research Initiative on Oceangoing Ships (2011). http://133.1.7.5/